Regionalization of sediment rating curve for sediment yield prediction in ungauged catchments

Sokchhay Heng and Tadashi Suetsugi

ABSTRACT

The main objective of this research is to regionalize the sediment rating curve (SRC) for subsequent sediment yield prediction in ungauged catchments (UCs) in the Lower Mekong Basin. Firstly, a power function-based SRC was fitted for 17 catchments located in different parts of the basin. According to physical characteristics of the fitted SRCs, the sediment amount observed at the catchment outlets is mainly transported by several events. This also indicates that clockwise hysteretic phenomenon of sediment transport is rather important in this basin. Secondly, after discarding two outlier catchments due to data uncertainty, the remaining 15 catchments were accounted for the assessment of model performance in UCs by means of jack-knife procedure. The model regionalization was conducted using spatial proximity approach. As a result of comparative study, the spatial proximity approach based on single donor catchment provides a better regionalization solution than the one based on multiple donor catchments. By considering the ideal alternative, a satisfactory result was obtained in almost all the modeled catchments. Finally, a regional model which is a combination of the 15 locally fitted SRCs was established for use in the basin. The model users can check the probability that the prediction results are satisfactory using the designed probability curve.

Key words | Lower Mekong Basin, regionalization, sediment rating curve, sediment yield, spatial proximity approach, ungauged catchment

Sokchhay Heng (corresponding author)
Tadashi Suetsugi
Interdisciplinary Graduate School of Medicine and Engineering,
University of Yamanashi,
4-3-11 Takeda,
Kofu,
Yamanashi 400-8511,
Japan
E-mail: *heng_sokchhay@yahoo.com*

INTRODUCTION

Sediment-observed data are lacking in many basins of the world, especially in developing and remote regions, due to institutional budget constraint (expensive observation), technical matter (difficult to measure, unfriendly samplers), etc. Although sediment is gauged in some areas, the sampling frequency is usually low (monthly or larger time scale). In most cases, only suspended load is measured and measurements of bed load transport are lacking. However, the suspended portion is predominant (Lu *et al.* 2012) and commonly account for about 90% of the total sediment flux (Walling & Fang 2003). Therefore, ungauged catchment (UC) in terms of sediment data is interesting.

As the finest fraction of suspended sediment load is often a wash load, it cannot be predicted well using stream power related sediment transport models (Asselman 2000; Warrick & Rubin 2007). Alternatively, empirical/data-driven techniques, e.g. sediment rating curve (SRC), are often taken into consideration (Jain 2012; Tayfur & Karimi 2014). SRC is an average relationship between discharge and sediment. It is commonly represented by power function. SRC is an important tool for the study of catchment hydrology. It can be applied to estimate sediment yield with known discharge (Zhang *et al.* 2012; Rosen & Xu 2013). Moreover, the rating curve itself informs physically the behavior of sediment erosion and transport processes (Asselman 2000; Horowitz 2003; Yang *et al.* 2006; Sadeghi *et al.* 2007). For example, steep rating curves characterize rivers where most sediment is transported at high discharge (Asselman 2000).

Prediction of hydrological variables for ungauged basins is still a great challenge to date (Saliha *et al.* 2011). After

doi: 10.2166/nh.2013.090

initiating the IAHS Decade on Predictions in Ungauged Basins scientific program (Sivapalan *et al.* 2003), many studies have been carried out to demonstrate the strategies and accuracy of UC modeling. The majority of them concentrate on streamflow prediction. In addition, regionalization of model parameters (parameterization) for UCs is often seen using catchment similarity, spatial proximity and regression approach. The catchment similarity approach transfers the parameter set from a modeled catchment having similar characteristics (climatic and physical) to the target UC. The spatial proximity technique uses the entire parameters from nearby gauged catchment with the rationale that catchments geographically close to each other should behave with similar characteristics. The regression method parameterizes the models in UCs using a relationship between model parameters calibrated on gauged sites and catchment attributes.

Oudin *et al.* (2008) compared these three regionalization approaches in the context of streamflow modeling by taking into account 913 catchments in France and found that spatial proximity provides the best regionalization solution. A similar study conducted in Austria by Parajka *et al.* (2005) and in Australia by Zhang & Chiew (2009) showed that spatial proximity is the most superior method. Some studies, e.g. McIntyre *et al.* (2005) and Oudin *et al.* (2008), have shown that using multiple donor catchments can reduce the uncertainty of model prediction in UCs. For output averaging method, output for the target UC is obtained by averaging results from the modeling using different parameter sets from different donor catchments. Another technique is parameter averaging in which parameter values of the target UC is computed as the mean of parameters from many donor catchments.

The main focus of this paper is to regionalize SRC for subsequent suspended sediment yield (*SSY*) prediction in UCs in the Lower Mekong Basin (LMB). The specific objectives are (1) to extract physical information containing in the locally fitted SRCs, (2) to evaluate the performance of SRC in predicting *SSY* in UCs, and (3) to compare the efficiency of the spatial proximity regionalization approach based on single and multiple donor catchments. Seventeen catchments are taken into account for the study. UC here refers to catchments having no sediment-observed data.

MATERIALS AND METHODS

Study area

The LMB covers about three quarters of the whole Mekong River Basin and its drainage area (around 606,000 km^2) is shared by four Southeast Asian countries: Lao PDR, Thailand, Cambodia and Vietnam. The LMB was selected as the study area because of the following reasons. The majority of the sediment gauging stations is concentrated in Thailand and ranked the highest with respect to data availability and completeness (Fuchs 2004), but many water resources development projects are planned in the other part of the basin. In total, there are 60 sediment monitoring stations in the LMB. If excluding those in the mainstream (14 stations), there are approximately 83% of the stations located in the basin part of Thailand. According to MRC (2011), there are currently 136 hydropower projects in which 26 are in operation, 14 are under construction and the remaining 96 (none in Thailand) are under planning. There are in total 4,129 planned irrigation projects and only 24% of them are located in Thailand. Therefore, establishment of a regional model (based on gauged catchments) for sediment prediction in UCs is feasible and very important for sustainable development in this basin.

The study area lies between latitudes 8°–23° N and longitudes 98° and 109° E with altitude varying from just over 2,800 m in the highland area of Lao PDR to zero at the coast in the delta in Vietnam (Figure 1). It is influenced by two main seasons, the rainy season (May–October) and dry season (November–April). The distribution of basin rainfall is primarily driven by topography as well as the general approach direction of the southwest monsoon and isolated tropical cyclones from the northeast across the South China Sea and Vietnam. The mean annual rainfall over the basin is greatly variable, ranging from less than 1,000 to more than 2,500 mm. Land use of the whole basin can be broadly divided into three main classes: paddy, forested land and land cultivated for field crops. Paddy (about 24% of the basin area) dominates the vast low-lying alluvial plains of the basin. The large majority of the basin part of Lao PDR and Cambodia is covered by forest, a mix of evergreen and deciduous types. Field crops are extensively found

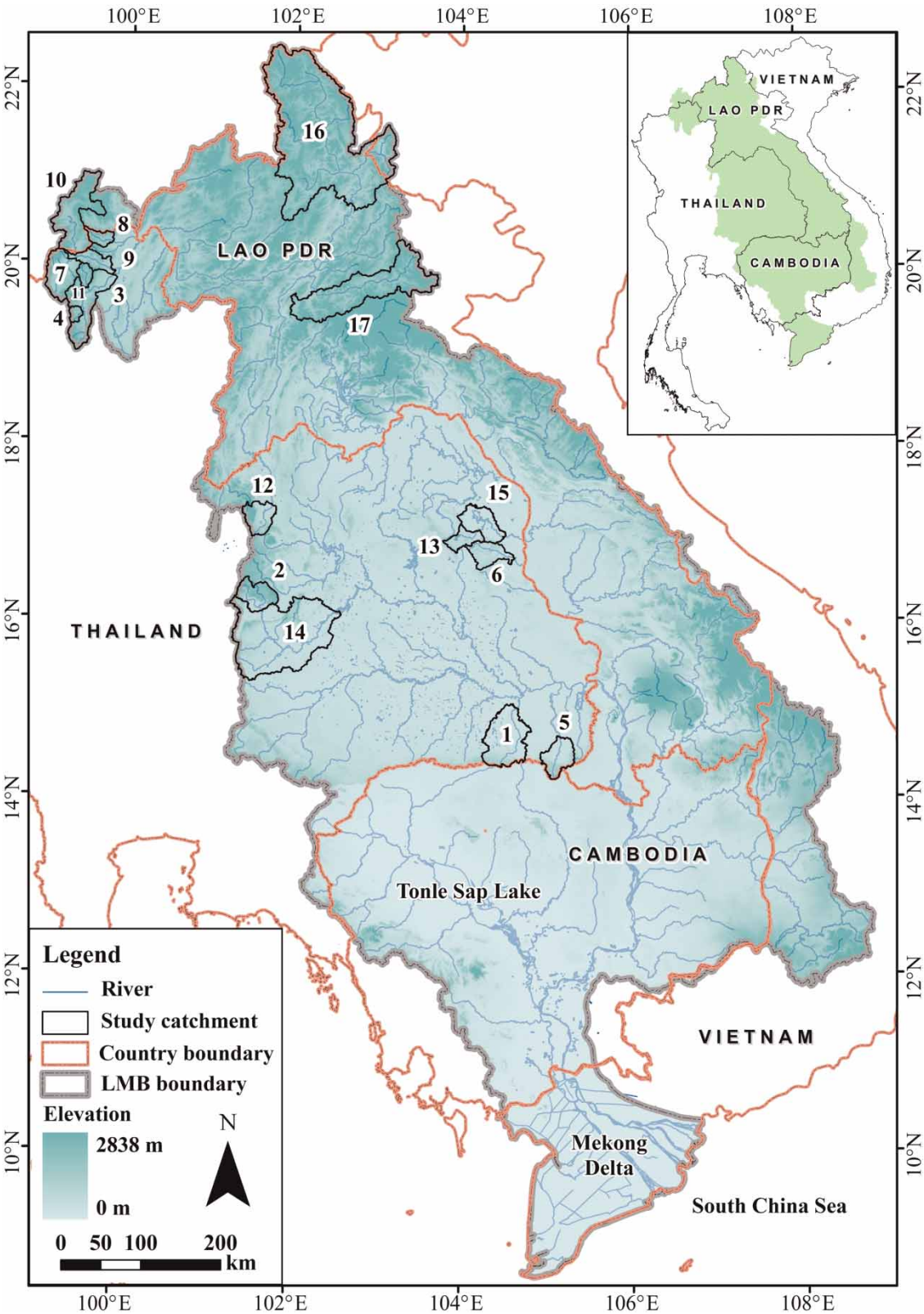

Figure 1 | Location map of the study catchments.

Table 1 | Summary of data and catchment characteristics

	T	N_{SSC}	A	SSY_a	Q_a	S
1	25	2	3,171	36	0.012	9.44
2	20	2	1,405	44	0.012	22.49
3	20	3	3,249	47	0.007	27.27
4	22	4	260	58	0.009	32.50
5	16	2	1,412	42	0.017	14.80
6	14	2	1,220	95	0.015	16.97
7	20	2	1,886	54	0.014	25.78
8	19	3	522	204	0.022	31.58
9	13	3	6,182	122	0.017	29.12
10	34	3	3,414	132	0.020	30.68
11	22	4	428	103	0.013	33.98
12	32	2	1,256	107	0.015	20.28
13	34	3	795	69	0.011	15.66
14	27	2	10,806	16	0.005	12.33
15	21	3	2,385	52	0.016	12.24
16	7	2	19,704	260	0.028	37.95
17	7	1	6,482	150	0.018	38.98

T (year): time length of available data; N_{SSC} (sample month^{-1}): monthly average sampling frequency of *SSC*; A (km^2): drainage area; SSY_a (t y^{-1} km^{-2}): annual *SSY*; Q_a (m^3 s^{-1} km^{-2}): annual discharge; S (%): catchment slope gradient.

within the gently sloping upland areas in Thailand. Acrisols are the most common soil type in the LMB overall and cover about 60% of the total drainage area. The second major type is cambisols (10.4%), mostly found along the river valleys in Lao PDR and Cambodia. Gleysols (7.7%) are commonly found in the Mekong Delta (Vietnam) and the inundated area of the Tonle Sap Lake (Cambodia).

Among 46 sediment gauging stations in the tributary rivers, only 17 (two in Lao PDR and 15 in Thailand) are candidates for the study because others contain only a few years of records with very low sampling frequency (less than one sample per month). The drainage catchment of each station was delineated using a digital elevation map (DEM). Characteristics of all 17 catchments are summarized in Table 1. The catchment area ranges from 260 km^2 of Catchment No. 4 (CAT4) to 19,704 km^2 of CAT16. The range of annual *SSY* (SSY_a) and discharge (Q_a) is 16–260 t y^{-1} km^{-2} and 0.005–0.028 m^3 s^{-1} km^{-2}, respectively. The catchment slope gradient varies from about 9.44% (CAT1) to 38.98% (CAT17).

Data

The main data used in this study are *SSY*, discharge (Q) and DEM. *SSY* is the product of Q and *SSC* (suspended sediment concentration). Daily data of *SSC* and Q were obtained from the Mekong River Commission (MRC). The reliability of the data was firmly controlled by MRC before releasing. The *SSC* sampling method and reliability discussion can be respectively found in Wang *et al.* (2009) and Walling (2005). The sampling procedures are based on the US practice and could reasonably generate samples for establishment of the mean *SSC* in the cross-section (Wang *et al.* 2009). The sampling equipment includes the point-integrating sampler of US P46/P61 and the depth-integrating sampler of US D49. The monitoring frequency is commonly low, ranging from one to four samples per month on average (Table 1). The uncertainty in load estimates at the 95% level of confidence is ±11.1–36.8%, ±4.6–13.8% and ±0.5–9.4% for monitoring frequency of one, two and four samples per month, respectively (Walling 2008). The data reliability and acceptability can be confirmed by their usage in many researches such as Kummu *et al.* (2010), Kameyama *et al.* (2013) and Shrestha *et al.* (2013). Due to the constraint of *SSC* datasets possessing only a few samples per month, the study was conducted on a monthly basis. Monthly time series of *SSY* and Q were applied for SRC fitting. DEM (30-m resolution) was downloaded from ASTER GDEM Version 2. ASTER GDEM is a product of METI and NASA. DEM was used for catchment delineation and determination of catchment slope gradient.

Sediment rating curve

The power form of SRC considered in this study is represented by

$$SSY = aQ^b, \tag{1}$$

where *SSY* (t day^{-1} km^{-2}) is the monthly *SSY* and Q (m^3 s^{-1} km^{-2}) is the monthly discharge. The rating coefficient (a) and the rating exponent (b) were estimated using nonlinear regression analysis of the power function. According to Asselman (2000), Horowitz (2003), Yang *et al.* (2006) and Sadeghi *et al.* (2007), a represents an index of soil erodibility

and b represents an index of river erosive and transport power.

Spatial proximity approach

The regionalization based on spatial proximity was applied to estimate model parameters in UCs. The hypothesis of this method is that nearby catchments should have similar behavior since climate and other catchment conditions should have minor difference spatially. The main concept of the spatial proximity approach is transferring the entire set of calibrated parameters from the closest neighboring catchment (termed as donor catchment) to the UC of interest. Donor catchment was searched by using the distance (D) between catchment centroids (Zhao *et al.* 2012). Each of the 17 gauged catchments where SRC was calibrated for were in turn treated as ungauged (termed as pseudo UC) for evaluation purposes. This procedure is also known as jack-knife validation.

Two alternatives were considered in this research. The first alternative is the utilization of a single donor catchment corresponding to the minimum D. The second one is the use of multiple donor catchments selected based on five different cases: (1) $D \leq 50$ km, (2) $D \leq 100$ km, (3) $D \leq 200$ km, (4) $D \leq 300$ km, and (5) all donor catchments. According to Parajka *et al.* (2005), cases 1–4 are called the local mean method and case 5 is the global mean method. Each case composes of two options. Option 1 is the output averaging in which SSY for month j was computed as

$$SSY(j) = \frac{1}{m}\sum_{i=1}^{m} SSY(j,\ \theta_i), \tag{2}$$

where m is the number of donor catchments and θ_i is the vector of parameters for donor catchment i. Option 2 is the parameter averaging in which SSY for month j was computed as

$$SSY(j) = SSY\left(j,\ \frac{1}{m}\sum_{i=1}^{m}\theta_i\right). \tag{3}$$

It is noted that both options are the same where m is equal to unity. This particular condition is equivalent to the first alternative, regionalization based on single donor catchment.

Catchment similarity approach

The catchment similarity-based regionalization approach was also tested so as to confirm its inferiority to the spatial proximity method. Here, the gauged catchment with the most similar characteristics to the target UC in terms of catchment descriptors was chosen as the donor catchment. The rationale of this approach is that catchments with similar attributes should behave similarly.

Four catchment descriptors (Table 1) were taken into account in this study: drainage area (A) in km^2, annual discharge (Q_a) in m^3 s^{-1} km^{-2}, catchment slope gradient (S) in %, and time length of available data (T) in year. Since catchment descriptors have different units and ranges, the rank-accumulated similarity was considered to select the donor catchment (Oudin *et al.* 2008; Zhang & Chiew 2009). For each descriptor, the most similar catchment to the target UC was assigned rank 1, the second most similar one was assigned rank 2, and so on. When multiple descriptors were applied, the ranks of the donor catchment for each descriptor were used to compute a mean rank. The catchment corresponding to the smallest value of the mean rank was then chosen as the donor catchment. It should be noted that each catchment descriptor has the same weight in this ranking system.

Model evaluation

As recommended by Moriasi *et al.* (2007), the model performance was evaluated by three statistical measures: Nash–Sutcliffe efficiency (NSE), percent bias ($PBIAS$), and ratio of the root mean square error to the standard deviation of observed data (RSR). For sediment modeling (monthly time step), the predictive accuracy can be judged as satisfactory in the case of $NSE > 0.50$, $-55\% < PBIAS < 55\%$ and $RSR \leq 0.70$. NSE, $PBIAS$ and RSR were calculated as

$$NSE = 1 - \frac{\sum (O-P)^2}{\sum (O - O_{\text{avg}})^2}, \tag{4}$$

$$PBIAS = 100 \times \frac{\sum (O - P)}{\sum O}, \quad (5)$$

$$RSR = \frac{RMSE}{SD_O} = \sqrt{\frac{\sum (O - P)^2}{\sum (O - O_{avg})^2}}, \quad (6)$$

where O is the observed SSY with the mean value O_{avg}, P is the predicted SSY, $RMSE$ is the root mean square error and SD_O is the standard deviation of the observed SSY.

RESULTS AND DISCUSSION

Fitted SRCs and their implications

The SRC of each catchment was fitted using the entire dataset available in each catchment and the results are summarized in Table 2. All SRCs exhibit a relatively good relation between Q and SSY with determination coefficient (R^2) ranging from 0.64 to 0.90. The steepness of the rating curve can be measured by the combination of a- and b-values since both coefficients behave in inverse correlation, b decreases with an increase in a (Figure 2(a)). If we fix the b-value, a steeper SRC corresponds to a lower a-value. The inverse correlation between the SRC parameters is due to the fact that the steeper catchments (in the north), having higher erosive and transport power (higher b-values), are dominated by forested lands having lower soil erodibility (lower a-values), in comparison with the more gently sloping catchments (in the central region) dominated by croplands (lower b- and higher a-values). In case all the study sites behave in a similar sediment transport regime (similar rate of sediment transport at both low and high discharges), there will be a strong correlation between a and b or the plotting locations between both parameters will be on the same line (Asselman 2000). Low values of R^2 are likely belong to steep SRCs, e.g. CAT8 ($R^2 = 0.64$, $a = 0.7111$, $b = 1.9975$). This is due to a wide scatter (Figure 3(a)) at high flow periods during which extreme events (e.g. slope failure, debris flow) might occur and cause large amounts of sediment in a short time. In addition, some measurements might be missed during large flood events while high sediment transports generally occur, and this leads to a small value of SSY while the corresponding Q is large.

Table 2 | Fitted SRCs and site-specific calibration results

	Fitted SRCs			Model performance		
Catchment	R^2	a-value	b-value	NSE	PBIAS (%)	RSR
1	0.86	4.5785	1.1529	0.62	9.60	0.61
2	0.75	1.9945	1.3662	0.68	29.35	0.56
3	0.90	4.9915	1.4318	0.87	10.63	0.37
4	0.72	1.7532	1.8382	0.67	16.31	0.57
5	0.84	2.9322	1.1672	0.68	19.82	0.56
6	0.86	2.7697	1.3759	0.61	29.45	0.62
7	0.83	5.8555	1.1597	0.68	10.24	0.57
8	0.64	0.7111	1.9775	0.53	20.98	0.69
9	0.79	2.3037	1.6322	0.76	9.27	0.49
10	0.72	1.1668	1.7518	0.65	14.75	0.59
11	0.64	1.0742	1.9018	0.77	23.53	0.48
12	0.85	2.8375	1.4622	0.79	20.69	0.46
13	0.85	2.2467	1.5425	0.75	15.95	0.50
14	0.86	6.3391	1.0793	0.74	2.85	0.51
15	0.89	4.993	1.1311	0.62	14.25	0.62
16	0.90	0.1672	2.231	0.40	− 1.45	0.78
17	0.79	0.7075	1.8809	0.76	24.41	0.49

The steepness of SRC could be used to describe river erosion and transport power and this can be confirmed by the good relationship between the rating curve parameters and catchment slope gradient (S) as depicted in Figure 2(b). Topography, represented by S in this research, physically governs the erosivity and transport capacity of the discharge (Heng & Suetsugi 2013a). This factor mainly drives sediment erosion and transport in a catchment. High erosive force and transport capacity of the discharge is corresponding to high flow velocity which usually occurs in steep slope terrain. In this study, both Q_a and SSY_a exhibit negative correlation with a and positive correlation with b. The flattest curve with the minimum value of Q_a and SSY_a in CAT14 (Figure 3(b)) implies that, in this catchment, the intensively weathered materials or loose sedimentary deposits are available for transportation at almost all discharges. The terrain in CAT14 is characterized by gentle slope gradient ($S = 12.33\%$), indicating low river erosive and transport power (low b-value). The predominant land use in this catchment is croplands, indicating high soil erodibility (high

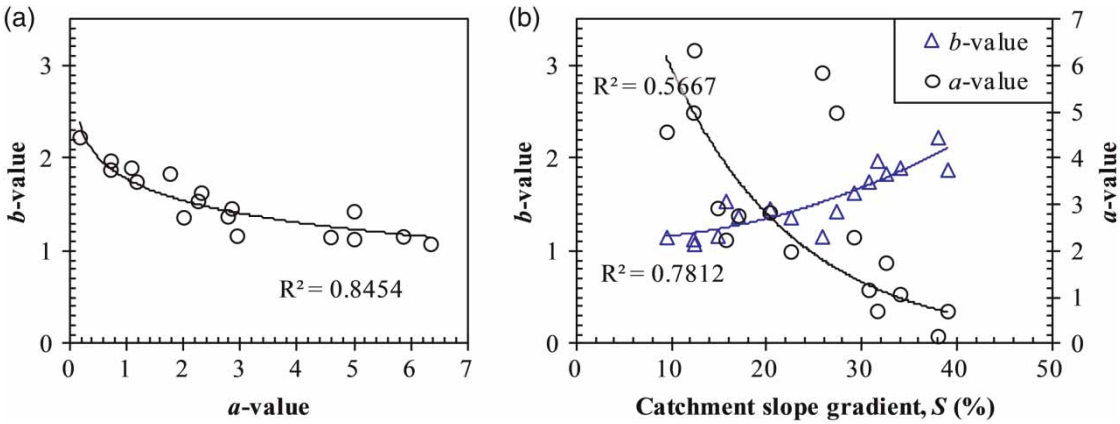

Figure 2 | (a) Inter-correlation between the SRC parameters and (b) their relationship with catchment slope gradient.

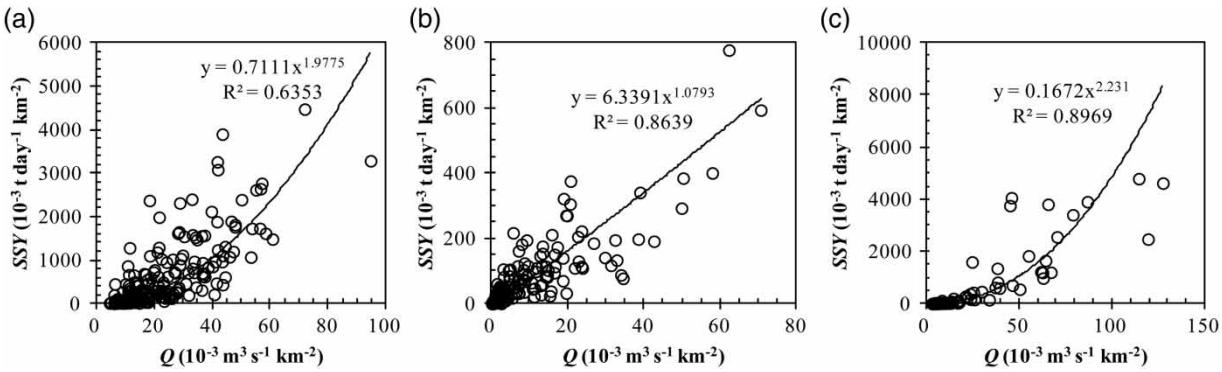

Figure 3 | Graphical illustration of SRC in (a) CAT8, (b) CAT14 and (c) CAT16.

a-value). On the other hand, CAT16 has the steepest rating curve (Figure 3(c)) with the maximum value of Q_a and SSY_a and this reveals that the erosive power to erode soil particles during high flow periods is significant. The topographic feature in CAT16 is mountainous ($S = 37.95\%$), reflecting the presence of steep river channels which produce high unit stream power with the potential for riverbed erosion and sediment transport (high *b*-value). Located in the Northern Highlands of Lao PDR, this catchment is covered mostly by forest, indicating low soil erodibility (low *a*-value).

The shapes (convex, linear and concave) of SRC could also be employed to infer specific hydrological factors/processes (Horowitz 2003). In this case study, there are no convex rating curves observed in all 17 catchments and this indicates that the river flows are not sediment-starved. It is suggested that the data used to construct SRCs have no effect from manmade hydraulic structures (e.g. dam-reservoirs) trapping the sediments. According to the Lower Mekong Hydropower database (MRC 2009), there were no hydropower dams operating in the study catchments during which the considered data were collected. The physical pattern of SRCs ranges from near linear (CAT14) to severe concave (CAT16). The linear curve represents the relationship between Q and SSY which does not change much during the considered period. The concave shape reveals that the re-deposited materials are transported coincidently with flows higher than those of the prior events eroding soil particles initially. This reveals that there is lag time between Q and SSY. Heng & Suetsugi (2013b) found that the average lag time is approximately 1.7 days in the LMB.

Calibration results

In the calibration stage, the fitted rating curve of each catchment (local SRC) was applied to estimate *SSY* in the same catchment (site-specific calibration) and its performance measured statistically by *NSE*, *PBIAS* and *RSR* is presented in Table 2. Except in CAT16, the predictive accuracy in the other 16 catchments is satisfactory with *NSE* ranging from 0.53 to 0.87 (median = 0.68), *PBIAS* from 2.85 to 29.45% (median = 16.13%) and *RSR* from 0.37 to 0.69 (median = 0.56). The difference in model efficiency could be explained by different nonlinear relationships governing spatial sediment erosion and/or transport processes. The low quality result in CAT16 could be due to significant variation of sediment transport temporally. This catchment is characterized by steep slope terrain ($S = 37.95\%$), and in consequence landslide or bank failure phenomena are important and possibly cause vast amounts of sediment load in a short time. Moreover, the enormous drainage area (19,704 km^2) and complex physical characteristics of the catchment might be the main factors leading to significant hysteretic effect (lag between *Q* and *SSY*) (Mikkelsen *et al.* 2013; Tananaev 2013) or the eroded materials require several events for transporting to reach the catchment outlet. Data uncertainty including measurement errors or low sampling frequency might also be the reason because CAT16 is situated in a remote mountainous area. For regionalization purposes, this poorly modeled catchment was not discarded because it can introduce a diversity that could be beneficial for modeling in UCs (Oudin *et al.* 2008).

Figure 4(a) shows an example of graphical comparison between the observed and predicted *SSY* (calibration stage) in CAT1. Both time series exhibit similar trends in all years. In the majority of catchments, over- and under-estimates are observed respectively for extreme low and high values. This is a common issue when the prediction is

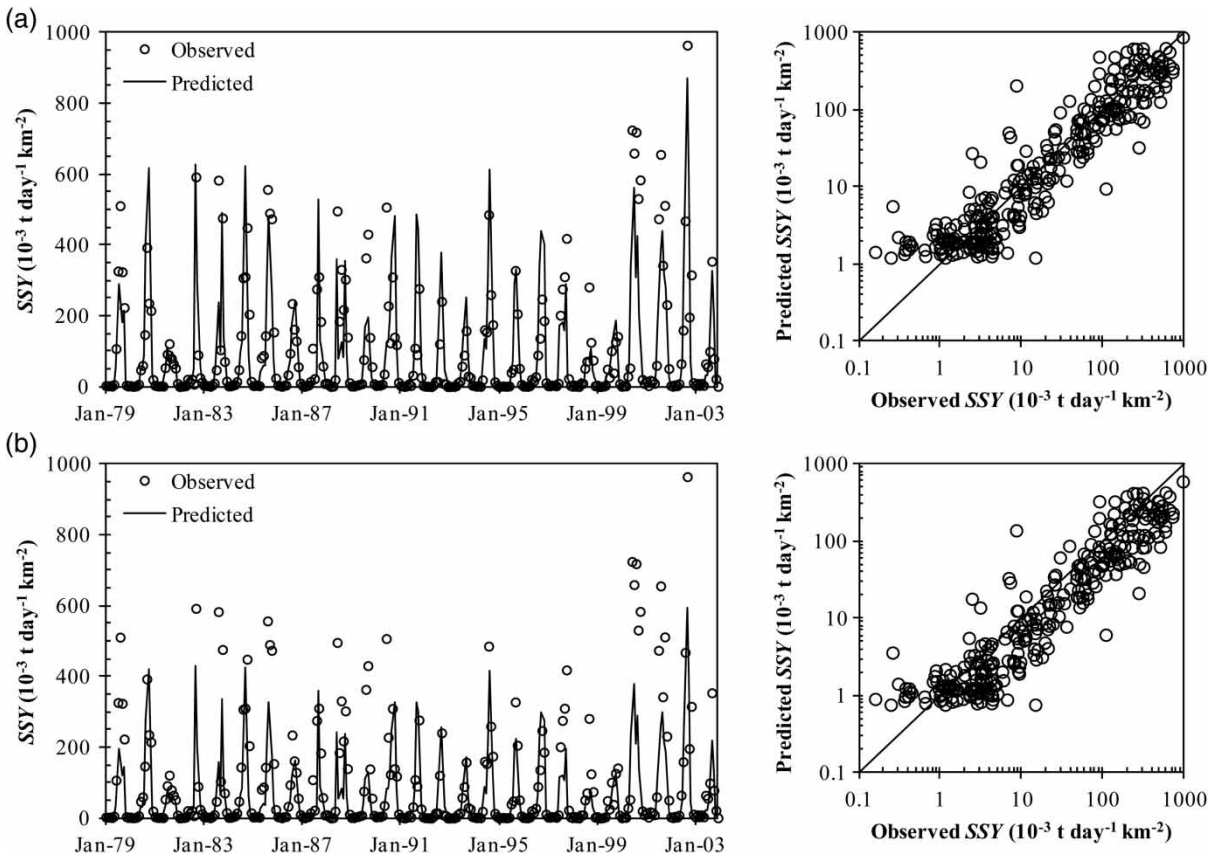

Figure 4 | Graphical comparison between the observed and predicted *SSY* in CAT1; (a) calibration stage and (b) validation stage (donor catchment is CAT5).

conducted using SRC because the model generally fails to encompass the entire events (Horowitz 2003; Zhang *et al.* 2012).

Prediction in UCs

The predictive accuracy in UCs was evaluated by jack-knife validation in which each gauged (modeled) catchment was in turn regarded as ungauged.

Spatial proximity approach

For the single donor catchment alternative, Table 3 presents the evaluation results (using 17 catchments) based on statistical measures. There are in total six unsatisfactorily modeled catchments (bold figures). Severe low accurate result ($NSE < 0$) is observed in CAT7 and CAT15. Negative *NSE* indicates that the observed mean value is a better predictor than the predicted value (unacceptable performance) (Moriasi *et al.* 2007). These two catchments have, respectively, CAT11 and CAT13 as the donor catchment. On the other hand, when CAT7 and CAT15 function as a donor of CAT6, CAT11 and CAT13, the predictive accuracies are not too low since *NSE* values are positive. Consequently, data uncertainty in CAT7 and CAT15 might be the main problem in this regard. As mentioned earlier, the sampling frequency of *SSC* is relatively low. Hence, in these two catchments, some measurements during extreme events (large amount of sediment transport) might be missed and this possibly causes a large error in generating the *SSY* datasets. The use of different sampling techniques in these specific sites could be a reason as well. To confirm, both CAT7 and CAT15 were suspended from the analysis. As the results in Table 3 show (using 15 catchments), the predictive accuracy in CAT6, CAT11 and CAT13 is improved significantly with new donor catchments and it also passes the minimum satisfactory criteria ($NSE > 0.50$, $-55\% < PBIAS < 55\%$ and $RSR \leq 0.70$). Accordingly, CAT7 and CAT15 were considered as outlier catchments and discarded from the study.

Table 3 | Site-specific model performance in UCs (validation results)

	Using 17 catchments					Using 15 catchments				
Catchment	**Donor**	***D*** **(km)**	***NSE***	***PBIAS*** **(%)**	***RSR***	**Donor**	***D*** **(km)**	***NSE***	***PBIAS*** **(%)**	***RSR***
1	5	70	0.54	39.18	0.67	5	70	0.54	39.18	0.67
2	14	51	0.67	16.59	0.58	14	51	0.67	16.59	0.58
3	4	21	0.85	1.26	0.39	4	21	0.85	1.26	0.39
4	3	21	0.64	20.03	0.60	3	21	0.64	20.03	0.60
5	1	70	0.67	– 18.56	0.57	1	70	0.67	– 18.56	0.57
6	15	35	**0.43**	**51.60**	**0.75**	13	36	0.53	– 13.06	0.69
7	11	30	**– 7.03**	**– 115.96**	**2.83**	–	–	–	–	–
8	9	32	0.54	24.42	0.68	9	32	0.54	24.42	0.68
9	10	31	0.69	31.13	0.56	10	31	0.69	31.13	0.56
10	9	31	0.61	– 9.94	0.63	9	31	0.61	– 9.94	0.63
11	7	30	**0.18**	**57.95**	**0.91**	3	32	0.54	19.60	0.68
12	2	98	**0.45**	**61.58**	**0.74**	2	98	**0.45**	**61.58**	**0.74**
13	15	20	**0.38**	**54.17**	**0.79**	6	36	0.57	42.30	0.66
14	2	51	0.71	27.76	0.54	2	51	0.71	27.76	0.54
15	13	20	**– 0.79**	**– 71.52**	**1.34**	–	–	–	–	–
16	17	198	0.63	4.35	0.61	17	198	0.63	4.35	0.61
17	16	198	0.76	30.68	0.49	16	198	0.76	30.68	0.49

Bold figures indicate unsatisfactory results; *D*: distance between catchment centroids.

Figure 4(b) illustrates graphically an example of comparison between the observed and predicted *SSY* (validation stage) in CAT1 whose donor catchment is CAT5. The predicted time series shows a similar trend with the observed one. The entire scattering points shift slightly downward of the ideal fit line, indicating underestimation of the whole range, from low to high value. This is due to the lower *a*- and higher *b*-value of the donor catchment. This condition is found similarly in CAT3, CAT6, CAT9, CAT14 and CAT17. The reverse condition is observed in other remaining catchments.

Spatial proximity versus catchment similarity approach

In the catchment similarity approach, CAT7 and CAT15 were also excluded from the analysis. By applying this method, the predictive accuracy is statistically summarized in Table 4. In comparison with the spatial proximity approach, catchment similarity was judged to provide less satisfactory results because of its higher uncertainty (larger range of *NSE*, *PBIAS* and *RSR*). Importantly, the catchment similarity method is also worse in terms of number of satisfactorily modeled catchment. This inferiority might be due to exclusion of other important catchment descriptors such as soil type which is a key physical descriptor in the context of this research (Oudin *et al.* 2008). The study did not consider the soil information in the regionalization process because of its unavailability. Another reason could be attributed to the weakness of the rank-accumulated similarity technique in searching the appropriate donor catchment.

Although the context of this research, sediment prediction and utilization of a simple model (SRC), is different from that of Parajka *et al.* (2005), Oudin *et al.* (2008) and Zhang & Chiew (2009), the results are in agreement. Therefore, it can be confirmed that spatial proximity provides a better regionalization solution than catchment similarity does.

The following sections present exclusively the analyses with regard to the spatial proximity approach.

Table 4 | Statistical comparison between the spatial proximity and catchment similarity regionalization approach

Approach	Indicator	Maximum	Minimum	Median	Pass
Spatial proximity	*NSE*	0.85	0.45	0.63	14
	PBIAS (%)	61.58	− 18.56	20.03	
	RSR	0.74	0.39	0.61	
Catchment similarity	*NSE*	0.83	− 0.06	0.57	10
	PBIAS (%)	70.13	− 70.19	13.19	
	RSR	1.03	0.42	0.66	

Pass: number of satisfactorily modeled catchments ($NSE > 0.50$, $-55\% < PBIAS < 55\%$ and $RSR \leq 0.70$).

Multiple donor catchments

The model performance for each case and option is listed in Table 5. For the output averaging option, the predictive accuracies are comparable among the first four cases (local mean method) with 0.57–0.60 of median *NSE*, 14.91–24.09% of median *PBIAS*, and 0.63–0.66 of median *RSR*. This is because the number of donor catchments is not significantly different between each case and/or catchments situated within a radius of 300 km may not behave very differently. In the case of $D \leq 50$ km, there are only eight feasible catchments and therefore a small amount (six) of satisfactorily modeled catchments. The significant poor results of the global mean method (case 5) could be explained by spatial catchment heterogeneity. Donor catchments located farther than 300 km might behave more differently (physical characteristics) from the target catchment and thus introduce large errors in the average output. Similarly, for the parameter averaging option, the four different cases of local mean method provide comparable results while the global mean approach is relatively inferior.

Output averaging versus parameter averaging option

There is no clear trend in judging which option is better than another. In terms of median *NSE* and *RSR* (Table 5), output averaging provides somewhat better results than parameter averaging in cases 2 and 4 but rather worse in cases 1, 3 and 5. In terms of median *PBIAS*, the output averaging option is relatively inferior to the parameter averaging one for all cases. However, the number of satisfactorily modeled catchments is slightly more numerous in the case of output averaging. If comparing the model efficiency catchment by catchment (Table 6), the parameter averaging option in general provides a larger amount of better modeled catchments.

Table 5 | Predictive accuracy of the output averaging and parameter averaging option

	Output averaging				Parameter averaging			
Case	***NSE***	***PBIAS* (%)**	***RSR***	**Pass**	***NSE***	***PBIAS* (%)**	***RSR***	**Pass**
Minimum D[a]	0.63	20.03	0.61	14	0.63	20.03	0.61	14
1. $D \leq 50$ km	0.57	17.14	0.66	6	0.58	16.36	0.65	7
2. $D \leq 100$ km	0.60	24.09	0.63	11	0.58	11.88	0.65	10
3. $D \leq 200$ km	0.57	14.91	0.66	12	0.57	4.35	0.65	11
4. $D \leq 300$ km	0.59	14.91	0.64	10	0.58	4.35	0.65	9
5. Global mean	0.46	13.49	0.74	7	0.50	1.63	0.71	7

[a]Single donor catchment; *NSE*, *PBIAS* and *RSR* are figured in median value.

Table 6 | Comparison between the output averaging and parameter averaging option in term of number of better modeled catchments

Indicator	**Minimum *D***	**Case 1 ($D \leq 50$ km)**	**Case 2 ($D \leq 100$ km)**	**Case 3 ($D \leq 200$ km)**	**Case 4 ($D \leq 300$ km)**	**Case 5 (Global mean)**
NSE	0–15–0	2–3–3	3–6–4	3–6–6	4–2–9	6–0–9
PBIAS	0–15–0	1–3–4	3–6–4	3–6–6	4–2–9	8–0–7
RSR	0–15–0	2–3–3	3–6–4	3–6–6	4–2–9	6–0–9

First value is the number of catchments where the output averaging option performs better; second value is the number of catchments where the output averaging and parameter averaging option perform equally; third value is the number of catchments where the parameter averaging option performs better.

Additionally, the number of better modeled catchments of both options increases at the same time when D (or number of donor catchments) increases. Its difference (3 = 9–6 or 1 = 8–7) in case 5, for instance, is likely not significant, and this reflects the inadequacy of sample size (number of catchments). Another factor which constrains this comparative study could be due to the sparse network of basin monitoring. Oudin *et al.* (2008) conducted a case study of streamflow prediction associating 913 French catchments (high density network of gauging stations). The results showed that the output average option is slightly more efficient because it employs the entire parameter set of the locally calibrated models.

Single versus multiple donor catchments

As shown in Table 5, regionalization based on single donor catchment apparently provides more efficient results than the one based on multiple donor catchments. Comparing with all five cases of the multiple donor alternative (both output averaging and parameter averaging), the single donor alternative is inferior in terms of median *PBIAS* but superior in terms of median *NSE* and *RSR*. In almost all catchments (14 among 15), the model performance passes the minimum satisfactory criteria. Although dissatisfaction was obtained in CAT12, the predicted value is still a better predictor than the observed mean value since *NSE* is greater than zero. To sum up, spatial proximity based on a single donor catchment provides the best regionalization solution. By using this alternative, *SSY* in UCs is predictable with accuracy in terms of *NSE* between 0.45 and 0.85 (median = 0.63), *PBIAS* between −18.56% and 61.58% (median = 20.03%), and *RSR* between 0.39 and 0.74 (median = 0.61).

Probability curve of predictive accuracy

Combination of all the 15 locally fitted SRCs (15 donor catchments) is hereafter called the regional *SSY* model. This model can be applied to estimate *SSY* in UCs in the LMB with known Q but its predictive accuracy will be unknown to users. In order to promote its application, it is necessary to provide a measure of model efficiency. A simple method is the utilization of a threshold on the D value to approximate a boundary between satisfactory and unsatisfactory model results. To achieve this purpose, a similar process of jack-knife validation was carried out but in

this case all potential donor catchments (14) were used alternatively for each target catchment (pseudo ungauged). There are in total 15 pseudo UCs and it corresponds to 210 pairs of the D value and model result. Based on regression analysis, the relationships between D and the statistical indicators (*NSE*, *PBIAS* or *RSR*) of the model efficiency are very weak (R^2 about zero). Therefore, it is impossible to determine a specific D threshold value.

Another technique which could similarly support the application of the regional *SSY* model is the probability curve of predictive accuracy. It is a relationship between D and the chance of obtaining satisfactory results (ratio of the number of satisfactorily modeled catchment to the total number of modeled catchments). The 210-sample size determined earlier was also used in this case. Figure 5 depicts the probability curve of predictive accuracy with respect to $NSE > 0.50$, $-55\% < PBIAS < 55\%$ and $RSR \leq 0.70$ (satisfactory model result). Explicit trend ($R^2 = 0.99$) is observed. The probability of obtaining a satisfactory result decreases with an increase in D value. The designed probability curve is so informative for the model users in measuring the possible predictive accuracy.

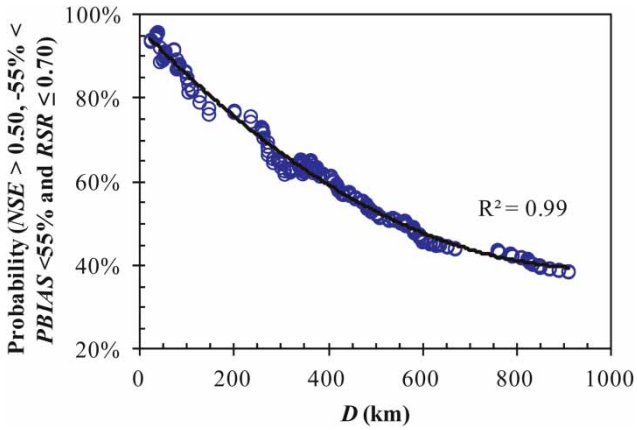

Figure 5 | Probability curve of predictive accuracy.

CONCLUSIONS

A power function-based SRC was fitted for 17 sites located in different parts of the LMB. The physical features of the fitted SRCs indicate that the eroded soil particles generally re-deposit and they might be transported to reach catchment outlets by several events. This suggests that clockwise hysteretic phenomenon of sediment transport is rather important in this basin.

The fitted SRCs were afterward applied to estimate *SSY* in UCs. Data uncertainty provoked extremely poor results in two catchments which were thus excluded from the analysis. The spatial proximity approach based on single donor catchment provides better regionalization solution than the one based on multiple donor catchments. By using the ideal alternative, a satisfactory result was obtained in almost all the modeled catchments and the predictive accuracy in term of median *NSE*, *PBIAS* and *RSR* is about 0.63, 20.03% and 0.61, respectively. We presently conclude that the simple SRC model is applicable in modeling *SSY* in UCs. However, there could be some uncertainties in the overall analysis because only 15 catchments were taken into consideration. Therefore, the findings in this paper remain debatable by future studies using a larger amount of catchments.

Last but not least, the established regional *SSY* model, which is a combination of the 15 locally calibrated SRCs, can be considered as a feasible tool in solving sediment-ungauged issues in the LMB. It is useful during the preliminary and feasibility study stage of water-related development projects while available data are generally very limited.

ACKNOWLEDGEMENTS

Immense gratitude is expressed to the Japanese Government (Monbukagakusyo: MEXT) and the Global Center of Excellence Program of University of Yamanashi, Japan, for supporting this research study. Sincerest thanks are extended to the Mekong River Commission for providing datasets.

REFERENCES

Asselman, N. E. M. 2000 Fitting and interpretation of sediment rating curves. *J. Hydrol.* **234** (3–4), 228–248.

Fuchs, H. J. 2004 Data Availability for Studies on Effects of Land-Cover Changes on Water Yield, Sediment and Nutrient Load at Catchments of the Lower Mekong Basin. Working Paper 09. MRC-GTZ Cooperation Programme, Göttingen.

Heng, S. & Suetsugi, T. 2013a Using artificial neural network to estimate sediment load in ungauged catchments of the Tonle Sap River Basin, Cambodia. *J. Water Resour. Protect.* **5** (2), 111–123.

Heng, S. & Suetsugi, T. 2013b Estimating quantiles of annual maximum suspended sediment load in the tributaries of the Lower Mekong River. *J. Water Clim. Chang.* **4** (1), 63–76.

Horowitz, A. J. 2003 An evaluation of sediment rating curves for estimating suspended sediment concentrations for subsequent flux calculations. *Hydrol. Process.* **17** (17), 3387–3409.

Jain, S. K. 2012 Modeling river stage-discharge-sediment rating relation using support vector regression. *Hydrol. Res.* **43** (6), 851–861.

Kameyama, S., Shimazaki, H., Nohara, S., Sato, T., Fujii, Y. & Kudo, K. 2013 Hydrological and sediment transport simulation to assess the impact of dam construction in the Mekong River main channel. *Am. J. Environ. Sci.* **9** (3), 247–258.

Kummu, M., Lu, X. X., Wang, J. J. & Varis, O. 2010 Basin-wide sediment trapping efficiency of emerging reservoirs along the Mekong. *Geomorphology* **119** (3–4), 181–197.

Lu, G., Wang, J., Li, Q., Zhao, J., Yu, M., Cai, T., Bai, X. & Xie, W. 2012 Impacts of Danjiangkou reservoir on sediment regime of the Hanjiang River. *Hydrol. Res.* **43** (1–2), 64–72.

McIntyre, N., Lee, H. & Wheater, H. 2005 Ensemble predictions of runoff in ungauged catchments. *Water Resour. Res.* **41**, W12434.

Mikkelsen, A. B., Hasholt, B., Knudsen, N. T. & Nielsen, M. H. 2013 Jökulhlaups and sediment transport in Watson River, Kangerlussuaq, West Greenland. *Hydrol. Res.* **44** (1), 58–67.

Moriasi, D. N., Arnold, J. G., Liew, M. W. V., Bingner, R. L., Harmel, R. D. & Veith, T. L. 2007 Model evaluation guidelines for systematic quantification of accuracy in watershed simulations. *Trans. Am. Soc. Agric. Biol. Eng.* **50** (3), 885–900.

MRC (Mekong River Commission) 2009 *Lower Mekong Hydropower Database*. MRC, Vientiane.

MRC (Mekong River Commission) 2011 Planning Atlas of the Lower Mekong River Basin. Report of the MRC. MRC, Phnom Penh and Vientiane.

Oudin, L., Andréassian, V., Perrin, C., Michel, C. & Le Moine, N. 2008 Spatial proximity, physical similarity, regression and ungaged catchments: a comparison of regionalization approaches based on 913 French catchments. *Water Resour. Res.* **44**, W03413.

Parajka, J., Merz, R. & Blöschl, G. 2005 A comparison of regionalization methods for catchment model parameters. *Hydrol. Earth Syst. Sci.* **9** (3), 157–171.

Rosen, T. & Xu, Y. J. 2013 Estimation of sedimentation rates in the distributary basin of the Mississippi River, the Atchafalaya River Basin, USA. *Hydrol. Res*. (in press).

Sadeghi, S. H. R., Mizuyama, T., Miyata, S., Gomi, T., Kosugi, K., Fukushima, T., Mizugaki, S. & Onda, Y. 2007 Development, evaluation and interpretation of sediment rating curves for a Japanese small mountainous reforested watershed. *Geoderma* **144** (1–2), 198–211.

Saliha, A. H., Awulachew, S. B., Cullmann, J. & Horlacher, H. B. 2011 Estimation of flow in ungauged catchments by coupling a hydrological model and neural networks: case study. *Hydrol. Res.* **42** (5), 386–400.

Shrestha, B., Babel, M. S., Maskey, S., van Griensven, A., Uhlenbrook, S., Green, A. & Akkharath, I. 2013 Impact of climate change on sediment yield in the Mekong River basin: a case study of the Nam Ou basin, Lao PDR. *Hydrol. Earth Syst. Sci.* **17** (1), 1–20.

Sivapalan, M., Takeuchi, K., Franks, S. W., Gupta, V. K., Karambiri, H., Lakshmi, V., Liang, X., McDonnell, J. J., Mendiondo, E. M., O'Connell, P. E., Oki, T., Pomeroy, J. W., Schertzer, D., Uhlenbrook, S. & Zehe, E. 2003 IAHS decade on predictions in ungauged basins (PUB), 2003–2012: shaping an exciting future for the hydrological sciences. *Hydrol. Sci. J.* **48** (6), 857–880.

Tananaev, N. I. 2013 Hysteresis effects of suspended sediment transport in relation to geomorphic conditions and dominant sediment sources in medium and large rivers of Russian Arctic. *Hydrol. Res*. (in press).

Tayfur, G. & Karimi, Y. 2014 Use of principal component analysis in conjunction with soft computing methods for investigating total sediment load transferability from laboratory to field scale. *Hydrol. Res*. **45** (4–5), 540–550.

Walling, D. E. 2005 Evaluation and Analysis of Sediment Data from the Lower Mekong River. Report of the Mekong River Commission. Mekong River Commission, Vientiane.

Walling, D. E. 2008 Sediment data for the Lower Mekong: a review of past monitoring activity. Paper presented at the Regional Workshop on Discharge and Sediment Monitoring and Geomorphological Tools for the Lower-Mekong Basin, Vientiane, October 2008.

Walling, D. E. & Fang, D. 2003 Recent trends in the suspended sediment loads of the world's rivers. *Glob. Planet. Change* **39** (1–2), 111–126.

Wang, J. J., Lu, X. X. & Kummu, M. 2009 Sediment load estimates and variations in the Lower Mekong River. *River Res. Appl.* **27** (1), 33–46.

Warrick, J. A. & Rubin, D. M. 2007 Suspended-sediment rating curve response to urbanization and wildfire, Santa Ana River, California. *J. Geophys. Res.* **112**, F02018.

Yang, G., Chen, Z., Yu, F., Wang, Z., Zhao, Y. & Wang, Z. 2006 Sediment rating parameters and their implications: Yangtze River, China. *Geomorphology* **85** (3–4), 166–175.

Zhang, Y. & Chiew, F. H. S. 2009 Relative merits of different methods for runoff predictions in ungauged catchments. *Water Resour. Res.* **45**, W07412.

Zhang, W., Wei, X., Zheng, J., Zhu, Y. & Zhang, Y. 2012 Estimating suspended sediment loads in the Pearl River Delta region using sediment rating curves. *Cont. Shelf Res.* **38** (15), 35–46.

Zhao, F., Chiew, F. H. S., Zhang, L., Vaze, J., Perraud, J. M. & Li, M. 2012 Application of a macroscale hydrologic model to estimate streamflow across Southeast Australia. *J. Hydrometeorol.* **13** (4), 1233–1250.

First received 18 May 2013; accepted in revised form 15 November 2013. Available online 27 December 2013